Research on Brain-Computer Interface-Based Unmanned Aerial Vehicle Control System

Jinghua Wang

Chang'an Dublin International College of Transportation at Chang'an University, Chang'an University, Xi'an, 710000, China
2023906043@chd.edu.cn

Abstract. Unmanned Aerial Vehicles (UAVs) are extensively utilized in both civilian and military sectors; yet, conventional UAV control algorithms encounter efficiency limitations in complicated situations. This research proposes a BCI-based UAV control system to enhance UAV control efficiency. This design system basically comprises a brain signal acquisition and processing module, a BCI control module, and a UAV flight control module. This design involves the acquisition of non-invasive electroencephalogram (EEG) signals, artifact removal via the Independent Component Analysis (ICA) algorithm, denoising through the Butterworth band-pass filter, and signal normalization using the Z-Score algorithm. The system operates on the Motion Imagery (MI) paradigm. The Fast Fourier Transform (FFT) algorithm is employed to extract signal features, while the Linear Discriminant Analysis (LDA) algorithm is utilized for classification. The training results indicate that the cross-validation accuracy of the LDA classifier in the test is 62.5%, demonstrating the design's efficacy and viability. The signal processing algorithm of BCI can be further refined in the future, facilitating the extensive implementation of this technology in the UAV sector.

Keywords: Unmanned aerial vehicle, brain-computer interface, electroencephalography, motor imagery

1 Introduction

Over the past decades, Unmanned Aerial Vehicles (UAVs) have been extensively utilized in both civil (commercial) and military applications owing to their cost-effectiveness, enhanced safety, versatility, portability, and enduring stability. Unmanned Aerial Vehicles (UAVs) are progressively supplanting piloted aircraft in executing jobs, particularly those of high danger, with extensive potential applications, including cargo transport, aerial photography, and synchronized operations. However, contemporary UAVs typically exhibit constraints regarding cargo capacity, operational range, and coordinated mission execution. In numerous practical applications, UAVs execute tasks jointly via UAV swarms. A fundamental issue in UAV swarms is navigation control, namely how to direct the UAVs to their destination via the optimal route while avoiding collisions with both static and dynamic objects [1]. Consequently,

J. Iqbal (ed.), *Proceedings of the 2025 2nd International Conference on Mechanics, Electronics Engineering and Automation (ICMEEA 2025)*, Advances in Engineering Research 272,
https://doi.org/10.2991/978-94-6463-821-9_85

the development of an effective UAV control system is crucial for the execution of UAV missions. Presently, the majority of UAV systems utilize PID control algorithms, Model Predictive Control (MPC) algorithms, and Linear Quadratic Regulator (LQR) control algorithms, among others, to achieve UAV system control. Nonetheless, these prevalent control methods typically exhibit drawbacks such as an extensive requirement for data-gathering samples, intricate computations, protracted planning durations, and limited real-time adaptability. Consequently, these UAVs are challenging to implement in a complex and changing operational environment, significantly diminishing both safety and efficiency in real applications [2].

In recent years, brain-computer interfaces (BCI) have facilitated advanced interaction across various domains while introducing a novel concept of control in drone technology. It directly interprets impulses from the human brain and transforms them into control signals for external equipment, so enabling commands to be issued to the devices through human awareness. This novel interaction mode can successfully surmount the inherent efficiency limitations imposed by the conventional UAV control approach. Consequently, numerous researchers in UAV system design have integrated BCI technology with UAV control technology, investigating various UAV control systems predicated on brain-computer interfaces and their associated control algorithms [3].

The brain-computer interface (BCI)-based unmanned aerial vehicle (UAV) control system comprises three primary components: the brain signal acquisition and processing module, the BCI control module, and the UAV flight control module. The review by Zhen, L. et al. (2023) identifies the predominant categories of acquired EEG signals as electroencephalogram signals (EEG), blood oxygenation signals (fMRI, fNIRS), and magnetoencephalographic signals (MEG) [4]. The primary BCI control paradigms include the Motor Imagery-based BCI paradigm (MI-BCI), the Steady State Visual Evoked Potentials-based BCI paradigm (SSVEP-BCI), the P300 Event-Related Potentials-based BCI paradigm (P300-BCI), as well as other BCI system paradigms and hybrid BCI system paradigms. In 2024, Beyrouthy, T. et al. examined the prevalent methodologies for evaluating data derived from brain signals, which encompass signal capture, preprocessing (including filtering, channel selection, and segmentation), feature extraction, and classification [5]. This work concentrates on the design research of UAV control systems utilizing BCI, based on the collection and processing of EEG signals and the design of BCI and UAV flight control systems.

2 Design of the BCI-Based UAV Control System

The BCI-based UAV control system shown in Fig. 1 primarily consists of a signal acquisition and processing module, a BCI control module, and a UAV flight control module. The comprehensive design concept of this system is as follows: first, identify the type of brain signals to be 11formulate the paradigm of the BCI control system; fourth, execute feature extraction and classification; fifth, perform signal decoding and control command mapping; and finally, devise the UAV control logic and algorithm.

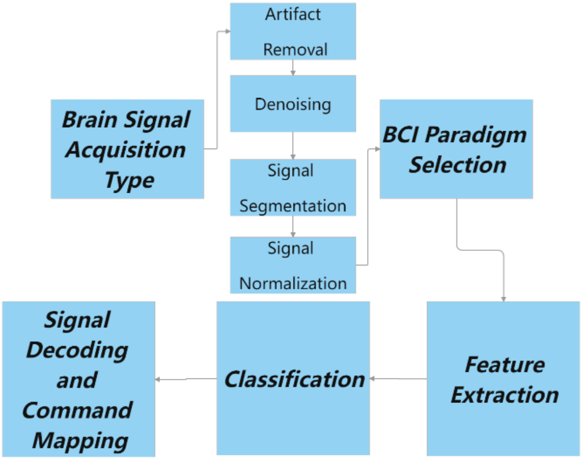

Fig. 1. Flowchart for the Design of BCI-Based UAV Control System.

2.1 Selection of Brain Signal Acquisition Type

The main techniques for acquiring BCI signals are classified as invasive and non-invasive based on the placement of the acquisition electrodes. While invasive BCI offers superior signal quality and accuracy compared to non-invasive BCI, it entails greater safety risks. Consequently, non-invasive BCI has been selected for this design. The brain signals obtained using non-invasive brain-computer interfaces (BCI) primarily include electroencephalogram (EEG), blood oxygenation level-dependent signals (fMRI, fNIRS), and magnetoencephalography (MEG) [4]. In comparison to other signals, EEG signals offer advantages such as low collection cost, rapid reaction speed, and high recognition resolution, establishing them as the predominant form of brain signals currently recorded. Consequently, the electroencephalogram signal (EEG) is designated as the signal acquisition type in this architecture.

2.2 Preprocessing methods for EEG signals

Artifact Removal. During the acquisition of EEG signals, the system is susceptible to external interference, forming various artifacts. These artifacts can cause great interference with the subsequent recognition and analysis of EEG signals, which leads to inaccurate classification results. Therefore, this design adopts the FastICA algorithm in independent component analysis (ICA) to remove the artifacts of EEG signals

According to Yang, C. et al.'s [6] review in 2021 in the FastICA algorithm based on maximum negentropy, the negentropy expression of the random variable is:

$$J(x) = H(x_g) - H(x) \quad (1)$$

where x_g is a random variable and x is a Gaussian random variable with the same covariance.

Since the probability density function of the random variable is unknown, the probability density function of the signal is usually estimated in terms of higher-order cumulants when solving the ICA problem, and the approximate expression for negentropy is:

$$J(x) \infty \left\{E\left[G(x) - E\left[G(x_g)\right]\right]\right\}^2 \tag{2}$$

where G(x) is a nonlinear quadratic function.

Since the essence of the algorithm is that the value of the negative entropy J (W^Tx) is maximized by choosing the appropriate transformation matrix W. When the variance is 1 and the mean is 0, solving for the maximum value of J (W^Tx) can be equated to finding the maximum value of E (GW^Tx). So before the algorithm starts, a preprocessing with two steps of centering and whitening is required. In this way, the problem can be transformed into solving for the maximum value of E(GW^Tx) under the condition that E(GW^Tx) = $\|W\|^2$ = 1. Calculation and simplification by Newton's method leads to the iterative equation:

$$W_{k+1} = E\{xg(W_k^T x)\} - E\{g^-(W_k^T x)\}W_k \tag{3}$$

where g(·) is the first-order derivative of G(·) and g^-(·)is the second-order derivative of G(·).

The algorithm can isolate one independent component after each iteration. Multiple independent components can be extracted after several iterations, and ultimately artifact removal from the EEG signal can be realized.

Signal Filtering and Removal of Linear Drift. Denoising procedures are typically necessary in the pre-processing of acquired MI-EEG data. The Butterworth bandpass filter, a widely utilized filter, exhibits significant stopband attenuation and a smooth passband accordingly. Consequently, it is frequently employed for the filtration of EEG signals. This system employs a Butterworth low-pass filter for signal filtration and the elimination of linear drift from MI-EEG signals.

Reviewed by Dipanwita, S. et al. [7], the gain of the Butterworth low-pass filter can be expressed in terms of the transfer function as:

$$G^2(w) = |H(jw)|^2 = \frac{G_0^2}{1 + \left(\frac{jw}{jw_c}\right)^{2n}} \tag{4}$$

where G(w) is the gain, G_0 is the DC gain or the gain at frequency 0, w is the angular frequency of the signal, w_c is the cutoff frequency of the filter, and n is the order of the filter.

Firstly, the cutoff frequency of the filter needs to be determined. Linear drift usually occurs in the low-frequency range, so an appropriate cutoff frequency can be selected in the medium-frequency range. Secondly, an appropriate filter order is selected and the transfer function is substituted, resulting in the design of the Butterworth filter. Finally, the filter is applied to perform signal filtering and linear drift removal on the acquired EEG signal.

Signal Segmentation. This architecture segments the acquired MI-EEG signals into predetermined time windows during the preprocessing stage to enable further feature extraction, analysis, and classification. To mitigate information loss, the segmentation procedure includes a certain percentage of overlap.

Signal Normalization. Reviewed by Borawski, M. et al. [8], the normalized index is:

$$Z = \frac{I_j - \bar{I}}{\sigma} \tag{5}$$

where Z is the standardized metric, I_j is the data point before standardization, $\bar{I}$ is the mean of the data set, and σ is the standard deviation of the data set. After normalization, the MI-EEG signal will have a variance of 1 and a mean of 0.

2.3 Paradigm design of the BCI module

This design employs motor imagery (MI) as the brain-computer interface (BCI) paradigm. The MI-BCI paradigm does not necessitate supplementary external stimuli to elicit EEG responses, unlike other BCI paradigms such as the P300 and SSVEP paradigms. Consequently, it offers the benefit of minimal implementation complexity; furthermore, the MI-BCI paradigm necessitates a reduced training duration, thereby lowering system development expenses; additionally, the MI-BCI paradigm is independent of target gaze, enabling system control despite visual impairment; moreover, the MI-BCI paradigm is less intrusive to the user compared to alternative BCI paradigms. Consequently, it offers an enhanced user experience [9].

2.4 Feature Extraction of MI-EEG Signals

In this design, the FFT (Fast Fourier Transform) algorithm is used for feature extraction of MI-EEG signals. Firstly, a suitable time window is selected according to the target time resolution or frequency resolution.

After that, to convert the time-domain signals into frequency-domain signals, the fast Fourier transform is applied to each window [10]:

$$X(f) = \sum_{n=0}^{N-1} x_n e^{-j2\Pi\frac{f}{N}n} \tag{6}$$

where x_n is the signal segment. Next, the power spectral density is calculated:

$$PSD(f) = |X(f)|^2 \tag{7}$$

Finally, the power spectral density is input to the classifier for the next step.

2.5 Classification

This design uses the LDA (Linear Discriminant Analysis) algorithm for signal classification [11]. First, the mean vector of each category of samples and the mean vector of all samples are calculated:

$$\mu_k = \frac{1}{N_k}\sum\nolimits_{x \epsilon C_k} x_n \tag{8}$$

where μ_k is the mean vector of category k, N_k is the number of samples in category k, k is the number of categories and C_k is the samples in category k.

$$\mu = \frac{1}{N}\sum_{n=1}^{N} x_n \tag{9}$$

where N is the number of categories, and μ is the mean vector of all samples.

Then, the intra-class scatter matrix and inter-class scatter matrix are calculated:

$$S_w = \sum_{k=1}^{k}\sum_{x_n \epsilon C_k} (x_n - \mu_k)\,(x_n - \mu_k)^T \tag{10}$$

where S_w is the intra-class scatter matrix, and N_k is the number of samples in category k.

$$S_B = \sum_{k=1}^{k} N_k\,(\mu_k - \mu)(\mu_k - \mu)^T \tag{11}$$

where S_B is the inter-class scatter matrix and N_k is the number of samples in category k.

Finally, the projection matrix W is solved with the formula:

$$W = argmax\left(\frac{W^T S_B W}{W^T S_W W}\right) \tag{12}$$

The eigenvalues are solved with the formula:

$$\lambda V_1 = S_w^{-1} S_b V_1 \tag{13}$$

where λ is the eigenvalue and V_1 is the eigenvector. All the eigenvectors are sorted by the size of the eigenvalues, and the projection matrix W can be formed by selecting the first k eigenvectors.

2.6 Signal Decoding and Command Mapping

At first, the category labels are established, and the appropriate control commands are tailored to these labels. The fresh signals are subsequently entered into the trained LDA classifier. Ultimately, the classifier can produce new signals as category labels and subsequently execute commands based on the correlation between feature labels and control commands.

3 Training of the BCI-Based UAV Control System

This design uses the open-source dataset BCI Competition IV Data Set 2a and uses the MI-EEG signal from it for this training [12].

The MI-EEG signal used for training has 22 EEG channels (0.5-100 Hz, with trap filtering), 3 EGO channels, a 250 Hz sampling rate, and 4 categories.

3.1 MI-EEG Signal Loading and Analysis

The MI-EEG signal was loaded and analyzed in MATLAB using the open-source toolbox EEGLAB (EEGLAB allows electrophysiological signal processing of loaded EEG data). EEG data stored in the specified folder in the file format GDF were loaded using the "op_biosig" function. After data loading, all EEG data were stored in an EEG structure for subsequent analysis and processing.

3.2 Downsampling Process

Use the "pop_resample" function to reduce the sampling rate of the data from the original value to 100 Hz, which not only improves the computational efficiency but also retains the key features of the signal.

3.3 Removal of MI-EEG Signal Artifacts Using the ICA Algorithm

The ICA analysis of the target EEG data is performed using the "pop_runica" function in EEGLAB, and "extended" is set to 1. Finally, the EEG data was observed in the EEGLAB window, and artifacts were removed from the data. The removal of artifacts was subsequently accomplished by removing the components related to eye movements and EMG using the "pop_subcomp" function.

3.4 Filtering of MI-EEG Signals Using Butterworth Band-Pass Filter

A Butterworth bandpass filter with a filter range of 0.5-40 Hz is used in MATLAB to remove the industrial frequency noise and the rest of the unwanted frequency components from the EEG data.

3.5 Normalization of MI-EEG Signals Using Z-Score Algorithm

The mean and standard deviation were calculated separately for the different channels of data, and the signal was subtracted from the mean divided by the standard deviation so that the data for each channel had zero mean and unit variance. Subsequently, all event types were converted from numeric to string form to ensure that each task event type was correctly recognized in subsequent processing.

3.6 Data Segmentation

Use the “pop_epoch” function to segment the EEG data according to the type of events extracted. Set the time window for each segmentation from -0.5 seconds (preparatory period) to 2.5 seconds (task execution period).

3.7 Extraction of MI-EEG Signal Features by FFT Algorithm

Using the “pwelch” function, the power spectral density of each channel is calculated by the FFT algorithm and log-transformed. The average power values of α-wave (8-13 Hz) and β-wave (13-30 Hz) are calculated separately and used as classification features.

3.8 Classification and Evaluation Using the LDA Algorithm

Train the LDA classifier using the “fitcdiscr” function to maximize the variance between and minimize the variance within EEG data categories.

3.9 Performance Evaluation of LDA Classifier

After training, the performance of the classifier was evaluated by k-fold cross-check validation using the “crossval” function [13].

3.10 Output of Control Instructions

Predictions were made for each trial using the trained model. Based on the output category of LDA, it is transformed into the corresponding flight control command

4 Evaluation of the BCI-Based UAV Control System Training Model

Two category labels, "Category 1" and "Category 2," have been established to denote "left-handed imagination" and "right-handed imagination," respectively. The two category labels are interpreted to produce the commands "UAV moves to the left" and "UAV moves to the right," respectively.

Utilizing 10-fold cross-validation, wherein 9 data subsets are employed for training and 1 subset serves as the validation set, the model undergoes this training and validation process 10 times, with each subset sequentially designated as the validation set. The resultant cross-validation loss of the model is 0.3750, indicating an average accuracy of 62.5%.

In addition, a simulation test was performed in this architecture utilizing a new set of EEG data from the BCI Competition IV Data Set 2a [12] dataset. Upon inputting the aforementioned EEG data into the model's LDA classifier and executing it via MATLAB, we acquired the subsequent results from 144 simulation tests:

Table 1. Results for 144 simulation tests.

Test number	Input label	Output result	Output correctness (%)
1, 2, 3, 6, 10, 11, 12, 13, 14, 16, 17, 18, 22, 25, 27, 29, 30, 31, 33, 34, 36, 37, 40, 41, 45, 49, 52, 54, 56, 57, 59, 60, 62, 63, 64, 65, 70, 77, 78, 79, 80, 83, 84, 87, 89, 90, 92, 97, 98, 100, 101, 103, 106, 108, 109, 111, 112, 113, 114, 119, 122, 123, 124, 127, 130, 131, 132, 133, 135, 136, 138, 141, 142, 144	Category 1	UAV moves to the left	100
4, 5, 7, 8, 9, 15, 19, 20, 21, 23, 24, 26, 28, 32, 35, 38, 39, 42, 43, 44, 46, 47, 50, 51, 53, 55, 58, 61, 66, 67, 68, 69, 71, 72, 73, 74, 75, 76, 81, 82, 85, 86, 88, 91, 93, 94, 95, 96, 99, 102, 104, 105, 107, 110, 115, 116, 117, 118, 120, 121, 125, 126, 128, 129, 134, 137, 139, 140, 143	Category 2	UAV moves to the right	100

The model attained 100% predictive accuracy over 144 simulation trials with a singular set of EEG data. It effectively differentiated between all left-handed imagery (category 1) and right-handed imagery (category 2), issuing the appropriate control commands ("UAV moves left" or "UAV moves right").

The cross-validation results indicate that the current model consistently exhibits stable performance across various training and testing data partitions, accurately predicting diverse datasets and demonstrating its stability and generalization capability over several data sets. The simulation test results indicate that the model can precisely recognize, forecast, and generate all control commands for a singular data set, hence confirming its accuracy with that specific data set. These two outcomes demonstrate the efficacy and practicality of this BCI-based UAV control system.

5 Conclusion

In this paper, detailed research and design of a BCI-based UAV control system is carried out. With the development of brain-computer interface (BCI) technology, its application in the field of unmanned aerial vehicles (UAVs) has brought a great breakthrough to the traditional UAV control method. By directly decoding and converting EEG signals into control commands, the BCI system can effectively improve the efficiency of UAV control. Combining the brain-computer interface technology with the UAV control system overcomes the efficiency bottleneck in the traditional control mode and, at the same time, promotes the development of UAVs in more complex application scenarios. Next, this paper presents and focuses on a BCI-based UAV control system design. The designed system mainly includes a brain signal acquisition and processing module, a BCI control module, and a UAV flight control module. In the signal acquisition part, the design chooses electroencephalogram (EEG) as the signal source. In addition, this paper describes in detail the preprocessing methods of EEG signals, including the use of the Independent Component Analysis (ICA) algorithm to remove artifacts, the use of the Butterworth band-pass filter for filtering and removing linear drift, and the use of the Z-Score algorithm for signal normalization. As for the design of the BCI control module, the design adopts the Motion Imagery (MI)-based BCI paradigm, which has the advantages of no need for external stimuli, short training time, and high adaptability. Finally, EEG signal features are extracted by the FFT algorithm, and signal classification is performed using the LDA algorithm. Subsequently, this paper details the training process of the designed system. The design uses the MI-EEG signal training model from the publicly available dataset BCI Competition IV Dataset 2a. As verified by the training results, the system with the LDA classifier performs well in predicting the results and can accurately recognize the mapping relationship between EEG signals and UAV control commands. This result illustrates the feasibility of brain-computer interface-based UAV control design, which can realize more accurate UAV control. Future research can be optimized in several directions. Firstly, the acquisition and processing algorithms of EEG signals need to be further improved to enhance the accuracy and stability of the control; secondly, more efficient BCI paradigms need to be developed to reduce the development time and cost of the system; and finally, with the advancement of BCI technology, the system in the future is expected to be widely used in UAV swarm collaborative tasking to improve the efficiency of UAV swarms. Overall, the BCI-based UAV control system proposed in this paper provides new ideas for the intelligent control of UAVs, especially in special environments or visually limited scenarios, which has important application value and potential.

References

1. Peng M, Meng W.: 'Cooperative Obstacle Avoidance for Multiple UAVs Using Spline VO Method', Sensors (Basel). **22**(5):1947 (2022)
2. Panlong, W., Fanjing, H., Shan, H., et al.: 'A review on unmanned aircraft system control', Electronics Optics & Control, **31**(10) :1-9 (2024)
3. Cheng, N., Phua, K., Lai, H., et al.: 'Brain-computer interface-based soft robotic glove rehabilitation for stroke', IEEE Transactions on Biomedical Engineering, **67**(12): 3339-3351 (2020)
4. Zhen, L., Zixing, L., Chao, R., et al.: 'A survey of brain-computer interface—based unmanned aerial vehicle control systems', Control Theory & Applications, 40f121: 2142—2159 (2023)
5. Beyrouthy, T., Mostafa, N., Roshdy, A., & Karar, S.: 'Review of EEG-based biometrics in 5G-IoT: Current trends and future prospects', Applied Sciences, **14**(2), 534 (2024)
6. Yang, C., Song X., Dezhi, L., et al.: 'The Application of Independent Component Analysis in Removing the Noise of EEG Signal'. 2021 6th International Conference on Smart Grid and Electrical Automation (ICSGEA), Kunming, China, pp. 138-14 (2021)
7. Dipanwita, S., Bhupati, M., Prasant, P.: 'A Review of the Filtering Techniques used in EEG Signal Processing'. 2023 7th International Conference on Trends in Electronics and Informatics (ICOEI), Tirunelveli, India, pp. 270-27 (2023)

8. Borawski, M., Biercewicz, K., Duda, J.: 'Determination of the Inaccuracies of Calculated EEG Indices'. Sensors (Basel). **20**(19):5715 (2020)
9. Maslova, O., Komarova, Y., Shusharina, N., et al.: 'Non-invasive EEG-based BCI spellers from the beginning to today: a mini-review', Front Hum Neurosci. Aug 23; 17:1216648 (023)
10. Mingyang, L., Wanzhong, C.: 'FFT-based deep feature learning method for EEG classification', Biomedical Signal Processing and Control, **66**, 102492, ISSN 1746-8094 (2021)
11. Melinda, M., Oktiana, M., Yunidar, Y., et al.: 'Classification of EEG signal using Independent Component Analysis and Discrete Wavelet Transform based on Linear Discriminant Analysis', International Journal on Informatics Visualization, **7**(3), 830–838 (2023)
12. ['BCI Competition IV: Datasets 2a', https://www.bbci.de/competition/iv/download/index.html?agree=yes&submit=Submit, accessed 03 July (2008)
13. Toleva, B., Atanasov, I., Ivanov, I., et al.: 'An effective methodology for diabetes prediction in the case of class imbalance. Bioengineering', **12**(1), 35 (2025)